Highly Optimizable Laminar Flow Control Devices

Johan Valentin Krier[1], Triyantono Sucipto[1]

[1]*IBK-Ingenieurbuero,*
Rehdorfer Str. 4, D-90431 Nuremberg, Germany
E-mail: *Johann.Krier@ibk-tech.de*, *Triyantono.Sucipto@ibk-tech.de*

Keywords: laminar flow control, attachment line contamination, anti contamination device, passive device

SUMMARY: The control of the flow gains importance due to the expected increasing fuel cost as well as environmental constraints. For the most aircrafts in service, the flow over the swept wings is turbulent in cruise conditions, partially due to the contamination experienced from the fuselage and partially due to given wing geometry configuration and flow conditions. In this paper several solutions for passive anti-contamination-devices (ACD) for laminar flow control, applicable for swept subsonic and supersonic wings are presented. The ACDs are capable to stop the spanwise propagation of fuselage-induced contaminated flow along the attachment line and to ensure the generation of a new laminar attachment line boundary layer. The first solution was originally developed for supersonic flow in the frame of the European Project SUPERTRAC, where it was also experimentally tested and proven to be effective. This solution is also suitable for existing aircrafts in service as "add-on" and it was extended for subsonic flow, too. The other two solution concepts of ACDs were developed later and are more suitable for new designed aircrafts. Numerical investigations were performed and presented for the last two. All three solutions have already been patented. Furthermore, the paper gives guidance for ACD-shape optimization. At the end, conclusions and outlook are drawn.

1 INTRODUCTION

Laminar flow technology (LFC) for aircraft gains more importance for cost and environmental reasons. Reduction of fuel consumption and noise level is the goal of LFC. As known, being laminar means less friction drag and lower noise level. In turn, less friction drag means less fuel burn and thus, less DOC and less CO_x and NO_x emission. The current paper deals with the development of a special class of passive devices for laminar flow control, the anti-contamination or de-contamination devices. Initial work was carried out within the European project SUPERTRAC and then continued inside of IBK. SUPERTRAC was the project addressing laminar flow control at supersonic flight regime. However, it is to underline that the application of the devices presented here are not limited to supersonic A/C but also usable for subsonic A/C.

The extent of laminar flow depends directly on the transition location on the surface of the body. It is thus the task of laminar flow control to delay the transition process as far backwards as possible. Two kinds of procedures are implemented in service which can sustain the laminar flow in natural way or by forcing it. The first – passive - is achieved by modifying the aerodynamic shape and the second – active - by using external energy for example to suck through, to blow over and to cool the aerodynamic surfaces in order to change or to control the airflow. The design of natural laminar wings is meanwhile a state of the art practice, even if in the aircraft world the number of existing aircraft with such wings is very limited. The benefit of having important laminar regions on different lifting or control surfaces depends also on the leading edge

contamination, a phenomenon extensive and deeply studied for several decennia [e.g. 1,2,3]. Leading edge flow contamination is a phenomenon of swept wings, in the way that the perturbations of the turbulent boundary layer of the fuselage are convected and propagated over the wing root along the attachment line on the wing leading edge in spanwise direction to the wing tip. The consequence is that the whole wing can be completely turbulent if the wave propagation is not damped i.e. beyond critical. This phenomenon can be controlled by the specific Reynolds number. For most A/C-swept-wings of practical interest, which are cruising at high subsonic speed as well as at supersonic speed, the attachment line Reynolds numbers are in most cases already beyond critical. Hereby, the risk of leading-edge contamination increases with increasing sweep angle. There are at least two known passive ways to reduce the contamination of the wing: by using micro-roughness distributions and by using anti- or de-contamination devices. The micro roughness distributions works by generating waves that damp the propagation of the turbulent perturbations. The effect is consequently a re-laminarisation of the initial turbulent flow. Anti contamination devices (ACD) eliminate the contaminated flow from the leading edge and initiate a new, healthy laminar flow behind the device. The contaminated flow is generally not "treated" (re-laminarised) by ACD, only removed from the leading edge and conducted downstream. In such case - in context of laminar swept-wing design - the ACD provides a solution to prevent the wing leading edge from being contaminated by the fuselage flow and also increases the working domain of the wing. Hence, the implementation of ACD for laminar swept wing is of great practical interest. In this relationship, the ACD can be implemented in conjunction with other laminar flow control methods such as flow suction or micro-roughness distribution. Fortunately, the ACD is just a small passive device which does not require complex mechanisms to be installed on the wing. Over there the design of ACD improved in the last time and is extensively controlled. Some questions regarding the design aspects are still open and will be outlined here. The classical example of ACD in the past was the 'Gaster bump' [3], that represents the non-optimized version of an ACD.

This paper deals with different aerodynamic aspects of anti contamination devices, which aim to be applicable for existing and new-designed aircraft, for subsonic as well as supersonic aircraft. Furthermore, some guidelines for optimizing ACD-shape and determining its parameters are also presented.

2 PROBLEM OF ATTACHMENT LINE CONTAMINATION

The phenomenon of attachment line contamination occurs when the turbulence convected from the fuselage to the wing and propagates along the attachment line of the leading-edge in spanwise direction and then spreads and contaminates the remaining flow over the wing surface. The parameter governing attachment line contamination is the attachment line Reynolds number $\overline{R}$. The spanwise propagation of the turbulence can be sustainable or damped if $\overline{R}$ is beyond or below a critical value, respectively. This matter had been extensively discussed in different papers (e.g. [1] [2]). The $\overline{R}$ was initially introduced for incompressible flow. For compressible flow, an adjustment is introduced and its corresponding Reynolds number is $\overline{R}^*$ which is defined by the following equation:

$$\overline{R}^* = W_e \frac{\eta}{\nu_e^*} \text{ with } \eta = (\nu_e^* / k)^{1/2} \text{ and } k = \frac{dU_e}{dx}$$

Here W_e is the velocity component along the leading edge, ν_e^* the local kinematic viscosity and k the velocity gradient (U_e and x in the plane normal to the leading edge). For quick prediction purpose, however, following a simplified-formula which is strictly valid for the case of the swept

infinite circular cylinder is often useful:

$$\overline{R}^* = \left[\frac{V_0 R}{\nu_e^*} \frac{\sin\varphi \tan\varphi}{2} \right]^{1/2},$$

where R is the leading edge radius, V_0 is the free stream velocity and φ is the wing sweep angle. Experiments had shown that leading edge contamination occurred as soon as the leading-edge Reynolds number exceeds a critical value of around 250. It was found, however, that the contamination could be delayed to a higher $\overline{R}^*$ if an effective anti-contamination-device was placed at the leading edge. Hereby, the anti contamination device has to fulfil the following **functional requirements**:

(1) To stop the propagation of the turbulent boundary layer flow along the leading edge attachment line.
(2) To initiate a new – not contaminated – attachment line flow behind the device.

These two functional requirements can be fulfilled by the most solution in the past, including the "Gaster bump".

From energetic and environmental considerations derives a supplementary requirement concerning the **optimization requirement**:

(3) To keep the disturbance induced on the wing by the presence of the ACD – upwards and downwards from the ACD – as low as possible. The disturbance should remain local and not promote early transition.

The third requirement is more pretentious and divides the ACD solutions in two categories:

a) ACD with its shape aligned to the flow pattern on the clean wing at the design point (the ACD body replaces a region of streamlines having the same geometry). The first two solutions in this paper are of this type.
b) ACD with its shape not being given by the flow pattern on the clean wing at the design point (its presence modifies essential the flow pattern at the leading edge). The typical exponent of this category is the Gaster bump.

The ACD of type a) can be easily and highly optimized, in comparison with the ACD of type b). These three requirements are not easy to be fulfilled simultaneously since many factors have to be considered, especially regarding local flow field pattern changes due to introduction of ACD.

3 DESIGN SOLUTION IDEA

Since the procedure for designing an ACD was initially not very well known, the search for an effective device started with simple shapes. The following steps have been exercised in SUPERTRAC:

- Study of existing ACD-shapes which are promising
- Analyzing some simple ACD-shapes and varying their ACD-heights
- Evaluating the results and develop a new shape as a solution idea based on the results.
- Verifying the solution idea and optimizing the shape.

The development of solution ideas to face with the above mentioned problem led to the following basic shapes of ACDs:

- Positive arrow-shaped ACD
- Negative arrow-shaped ACD
- Split-ACD

All mentioned shapes will be elaborated in the next chapters. The solutions are aimed to be applicable for existing and new-designed aircraft, for supersonic as well as for subsonic aircraft. The first one was initially designed for SUPERTRAC-Project and its effectiveness has been tested successfully in the S2-Onera supersonic wind-tunnel. Its shape has been, however, further

modified and improved. The later two are own-developments and have been only numerically analyzed.

4 NUMERICAL AND EXPERIMENTAL ANALYSIS

4.1 *Numerical approach in SUPERTRAC*

For evaluation purpose, the numerical fully RANS-method was used. The unstructured solver TAU-code (by DLR) with the Spalart-Allmaras turbulence model was implemented to solve the RANS equations, while the required hybrid grids were generated using CENTAUR. It was however realized that the RANS codes have no capability to predict a reverse transition i.e. re-laminarisation since the implemented turbulence models generate an a priori turbulence. However, for reasons given in detail in chapter 5.1 a RANS-solution is sufficient for the design.

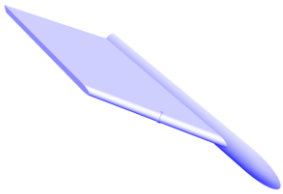

Figure 1: Geometrical model

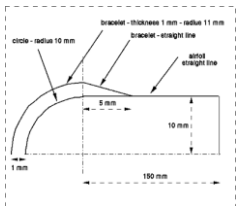

Figure 2: ACD-reference shape

The platform for numerical modelling of ACD-simulation was a simple swept wing and a dummy fuselage on the wing root for enabling simulations of flow contamination by fuselage (*fig. 1*). The wing was just a thick and swept plate with a half-cylinder leading edge. The ACD was placed in the midspan of the wing. As mentioned before, some simple ('standard') shapes were exercised in the beginning with the purpose to understand the physics of leading-edge contamination and provided guidance to design an effective ACD. A rectangular shape ACD (bracelet) was generated as a reference, shown in *fig. 2.* This bracelet had a 5 mm width and a 1 mm height. The flow condition for numerical analysis was intentionally chosen for the case which would provide sufficient flow contamination. This was carried out by using a proper $\overline{R}*$ beyond the critical value. A supersonic speed was considered since the ACD was initially developed within the SUPERTRAC project. The main flow parameters were: wing-sweep angle φ=65°, leading-edge radius R= 10mm, Mach number M= 1.7, total temperature T_t = 300 K, total pressure p_t =1.4 bar. This condition corresponds to $\overline{R}*$=443.

Later, having received the results from the wind tunnel test, existing ACD-shapes were further optimized and new ACD-shapes were introduced and analyzed. The flow conditions were extended to cover both subsonic and supersonic speeds. *Table-1* shows the flow conditions for follow-up numerical analyses.

	Supersonic	Subsonic
Wing sweep, φ	65°	37.3°
Leading-edge radius, R	6 mm	6 mm
Mach number, M	1.7/2.7	0.85
$\overline{R}*$ or p_t	variable	variable
Total temperature, T_t	300K	300K

Table-1: Flow conditions for follow-up analyses

4.2 *Solution of positive arrow-shaped ACD*

The above considerations led to a construction of a trapezoidal ACD of 5-mm height with cylindrical nose, to stop the contaminated flow, and followed by streamlined “legs” to avoid disturbances. These combinations delivered a unique ACD-shape, an arrow-shape. In this case, the device protrudes from the wing surface and is thus termed as ‘positive’ arrow-shaped ACD and named as "ACD5". This ACD-shape was designed to give solutions to the problem formulated in the previous sub-chapter. *Fig. 3* shows the ACD-shape concepts.

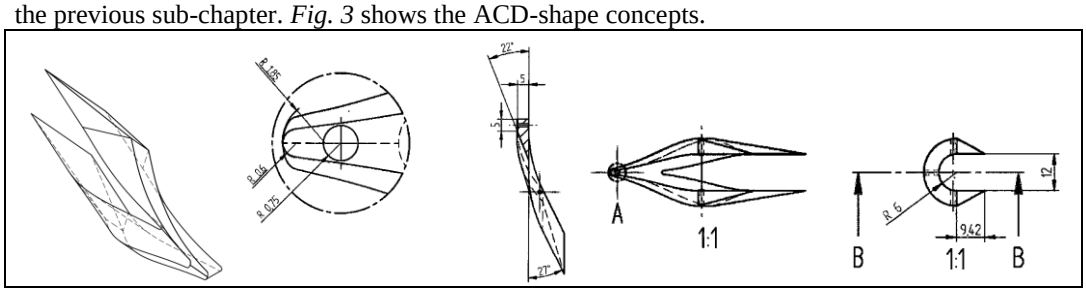

Figure 3: ACD5-concept

For this ACD5 wind tunnel experiments were conducted in frame of the SUPERTRAC-Project by Onera at Onera-S2MA facility. ACD5 was one of totally 7 ACD-shapes, being experimentally investigated. Other shapes were either simple shapes (rectangular, trapezoidal, streamwise parallelepiped) or special shapes proposed by other partners of SUPERTRAC-Project. During the tests, the ACDs were placed on the leading edge of a 2.5D-Onera-wing platform which is swept for 65 degrees. It had a symmetrical profile with 6 mm-leading edge radius. The tests for the ACD were made for Mach 2.7 and 1.7 (supersonic and subsonic leading edge, respectively). The efficiency of the ACD was evaluated by three hot films located upstream (HF1) and downstream of the ACD (HF2) and near the wing tip (HF3). Via hot films, signals of disturbances could be recorded in form of RMS-values. The level of RMS values would then reveal the state of the flow whether laminar or turbulent. For both Mach numbers M=1.7 and M=2.7, the $\overline{R}*$ were varied by increasing the total pressure from 0.3 bar up to a sufficient upper value where the investigated device was no longer effective. It is worth to know that by maintaining the total pressure, the $\overline{R}*$ decreases as the Mach number increases. The records of RMS-level distributions are presented in *fig. 4* for both Mach numbers as a function of $\overline{R}*$. The three diagrams in each unit represent RMS-levels from hot-film HF1 (locations before ACD, top diagram), HF2 (just after ACD, mid diagram) and HF3 (close to tip, bottom diagram). It is clear from these figures that ACD5 exhibits the best performances. The onset of leading edge contamination is delayed up to $\overline{R}*$ = 330 at M = 1.7 (total pressure P_t = 0.5 bar) and $\overline{R}*$= 400 at M = 2.7 (P_t = 1.2 bar). The other ACD’s did not show any clear effectiveness.

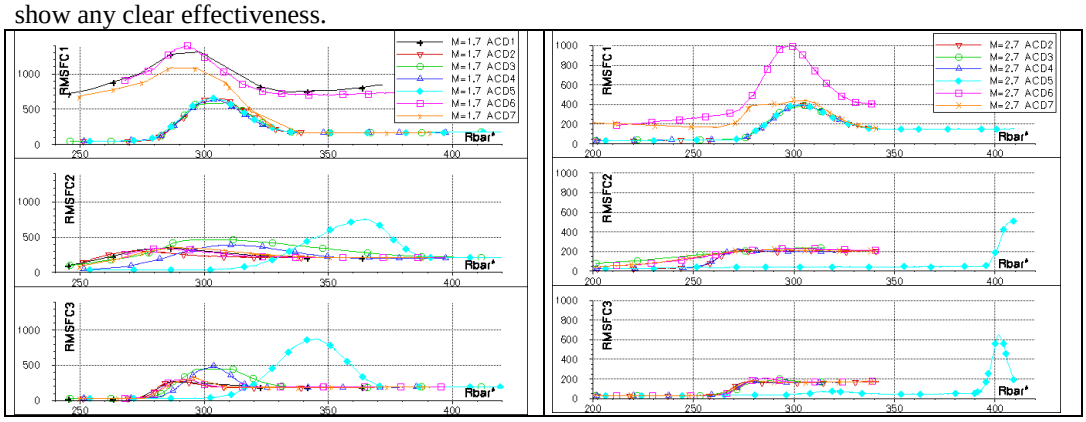

Figure 4: Experimental results of ACD investigation

Having studied the experimental results, it was apparent that not all ACD-shapes could work well. It could be deduced that it was not easy to design an effective ACD. However, the experiment had delivered some valuable information about the way of designing an effective ACD, for example regarding its shape and height. Having got the results from the wind tunnel tests, follow-on computations on ACD5 were carried out. The existing ACD5 shape was further optimized in the way that it became more streamlined. The ACD5 was this time mounted on the similar wing with 6 mm leading-edge radius (it corresponded to the wing leading-edge radius used during the WTT).

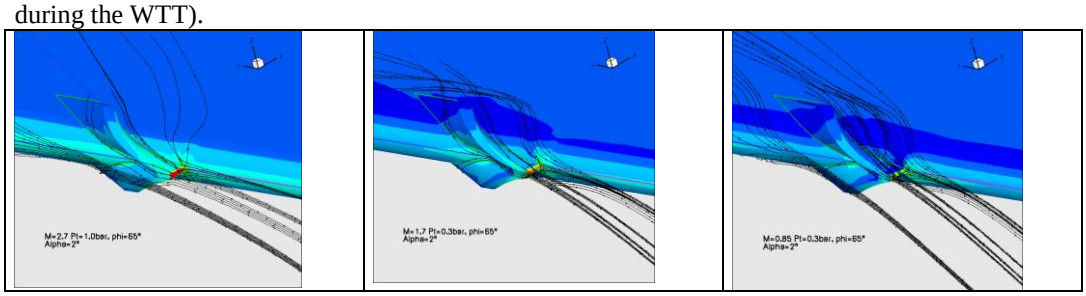

Figure 5: Follow-up analyses on ACD5

The ACD5 was then analyzed for supersonic as well as for subsonic cases. Furthermore, angle of attack variations were also exercised. Exemplary results for pressure coefficient and streamlines for α=2° ratios are shown in *fig. 5*. The results showed that the streamlines over ACD were smooth in general and the disturbance remains small, also at off design condition.

4.3 *Solution of negative arrow-shaped ACD*

'Negative' arrow-shaped ACD refers to the device which intrudes and cuts away the wing surface locally. It was the experimental result which revealed the negative ACDs were able to minimize the generation of disturbances, but did not affect the de-contamination process.

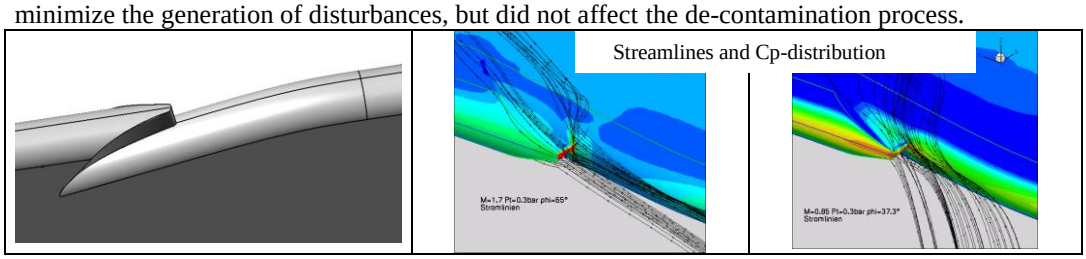

Figure 6: Negative-ACD and exemplary numerical results

Thus, taking advantage of arrow-shaped ACD, a negative arrow-shaped ACD was designed. This kind of ACD is expected to minimize the local disturbance but remains effective. It is practically another ACD5 in negative (inward) direction. *Fig.* 6 shows the geometry of the new negative-ACD and exemplary results at M=1.7 and M=0.85. The streamlines, local pressure coefficient and viscous ratio distributions comply with the common characteristics mentioned before and promise even better characteristics (i.e. less disturbances at expected comparable effectiveness).

4.4 *Solution of split ACD*

The third ACD solution is a new idea of ACD. It is a split ACD and shown in *fig. 7*. The device splits the incoming flow at wing root leading edge and conducts it downstream on the upper and lower wing surface with minimal resistance. The contaminated fuselage flow is thus

prevented from ever being propagated to the wing spanwise. For this purpose the ACD is made to have a sharp leading edge and has no sweep to free stream. The preliminary analysis results are shown. It is carried out intentionally for high subsonic Mach number M=0.85 to show that this kind of ACD is expected to be applicable for subsonic regime. The streamlines, pressure coefficient and viscosity ratio distributions have shown that the device is promising to be effective. However, the device is still subject of further investigations for low-speed flight conditions.

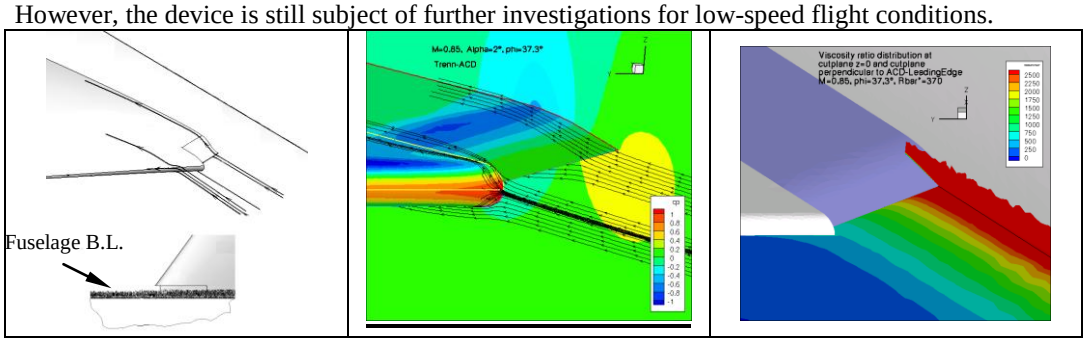

Figure 7: Split-ACD, functionality and exemplary analysis result

4.5 *Implementation to the A/C*

Practical implementations of the ACD could be on the design of new laminar A/C-wing. Apart from that it can also be implemented as add-on on existing aircrafts in service. Despite of turbulent wing design of most of existing A/C-wings, there is reasonable possibility to develop flow laminarity to up to 5% of wing chord within slat area. If the full-turbulence of the wing is caused by flow contamination, there is a chance for ACD-implementation to produce small laminar region. As known, a small drag reduction is already significant for saving operating cost as well as saving emission and noise. The ACD5, for example, is a small device which can be implemented as add-on on the existing wing with small wing modification. The negative-ACD is more difficult to implement as add-on, meanwhile the split-ACD could be only viable for new laminar aircraft wings.

An example of an ACD5-implementation on 3D-A/C-laminar wing is presented. Preliminary numerical investigations were carried out with the goal to evaluate the extent of disturbance created by the ACD. Both configurations of clean wing as well as wing with ACD5 were considered for comparison. Investigations were limited to inviscid Euler-simulations. The results are shown in *fig. 8*.

Two conditions at different angle of attack, namely at C_L=0.11 (on-design point) and C_L =0.18 (off-design point) were exercised. Since the real wing leading-edge was no longer cylindrical, its ACD-installation was also not trivial. The ACD5 had then been redesigned.

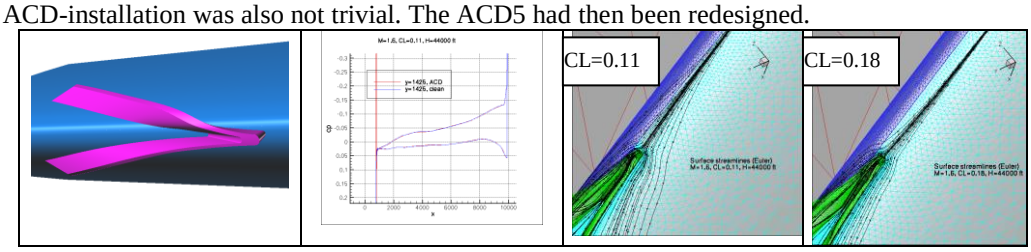

Figure 8: Example of ACD5 implementation on 3D-A/C laminar wing

The figure of the pressure coefficient distributions reveals that the existence of ACD5 practically does not change the global pattern. At the upper and lower wing surface the global patterns of Cp for clean wing and wing-ACD5 are indeed very similar. However, local disturbance

occurs at the surrounding of ACD. Away from ACD the disturbance is fully damped. At off-design condition C_L =0.182, the wing-leading-edge streamlines upstream of the ACD are bent and guided to the ACD-leading-edge. This phenomenon reduces strongly the effect of small angle of attack variation about the design-angle of attack. Cp-disturbance due to ACD-existence at off design is also less significant and does not change the global picture.

5 SHAPE-OPTIMIZATION

Shape optimization guidelines are presented for practical use to design an effective ACD. First, basic principles or criteria of ACD designs are introduced. Then, basic parameters are briefly discussed.

5.1 *Basic Principles of ACD Design*

The attachment line transition laminar to turbulent occurs at a critical value $\overline{R}^*$ of about 250±35. If the value is lower, the boundary layer at the leading edge remains laminar and becomes contaminated as $\overline{R}^*$ gets higher than the critical value. If the flow is contaminated at the leading edge, the question of "de-contamination" or "re-laminarisation" comes up. Both are two different terms, due to the fact that a de-contamination implies only stopping and evacuating of contaminated leading edge flow, whereas a re-laminarisation implies a change of state of the leading edge flow (damping of turbulences). The problem of anti-contamination is apparently a local problem of de-contamination although it is often miscalled as re-laminarisation. In case of ACD, the appearance of a new, laminar boundary layer at leading edge downwards of ACD is not a consequence of flow-transformation induced by ACD but it comes from undisturbed flow at upstream of the wing which is aligned to the de-contaminated leading-edge downwards of ACD. Thus, the use of RANS methods is justified and completely sufficient, since a simulation of re-laminarisation process is not stringently required. The quality of an ACD can then be evaluated by its generated disturbances. This kind of evaluation can be carried out by standard RANS-method. The capability to simulate re-laminarisation or inverse transition – which is beyond the capability of standard RANS-method – can be circumvented, then. In this paper, only the de-contamination problem is being considered. As already mentioned in section 2., the ACD-problem consists of three aspects: 1) stop and evacuate the incoming contaminated boundary layer, 2) laminar (de-contaminated) flow arises downward of ACD and 3) the disturbances in correlation with the device is reduced to a minimum. While the first two requirements represent the functionality of the device, the last problem constitutes an optimization problem.

First problem can be solved by (almost) any physical body, which is placed directly on the attachment line and has a sufficient height (necessary height depends on its form). As an example, a circular cylinder with a radius of 1/10 of the leading edge radius can be used. This solution does not necessarily fulfil the second requirement, because past of cylinder a massive flow separation field with high turbulence occurs, which most likely contaminates the new flow downward of the cylinder (*fig. 9* left).

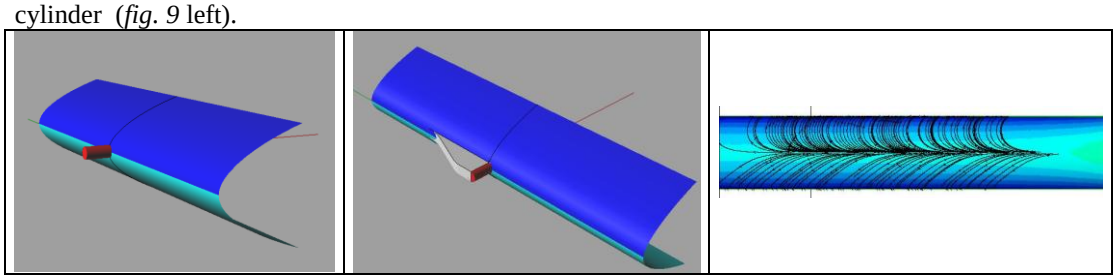

Figure 9: Basic idea of ACD-shape design

To fulfil the second requirement, the body should enable a smooth downward flow. This requires a top plateau, followed by a sloped rear surface (*fig. 9* mid). Nevertheless, such body is still not fulfilling the third requirement since there will still be flow separations on the both sides (left/right) of the body. Solutions for the decontamination problem that fulfil all these three requirements have to consider the streamlines (or friction line at surface) at the leading edge of the undisturbed (clean) wing (*fig. 9* right). Apparently, any solution which does not induce large interference to the existing flow, should take a form that conforms to existing stream- or friction line pattern. In other words the surfaces of the device should be streamlined by the pattern of the clean wing. However, in practice it is not easy to achieve and build a device, which persistently fulfils these requirements at a range of flight conditions. Due to this fact, off-design characteristics have to be taken into account. All of the above mentioned ACDs – developed by IBK – were designed according to these basic principles. The first one, the positive arrow-shaped ACD5, has already been experimentally proven to be effective and fulfilled all three requirements. The other ones, the negative arrow-shaped ACD and the split ACD are also expected to fulfil these requirements too.

5.2 *Determination of main parameters*

In this paper, an analytical-empirical method is presented to determine the main parameters of an ACD. As reference, the positive arrow-shaped ACD5 is used.

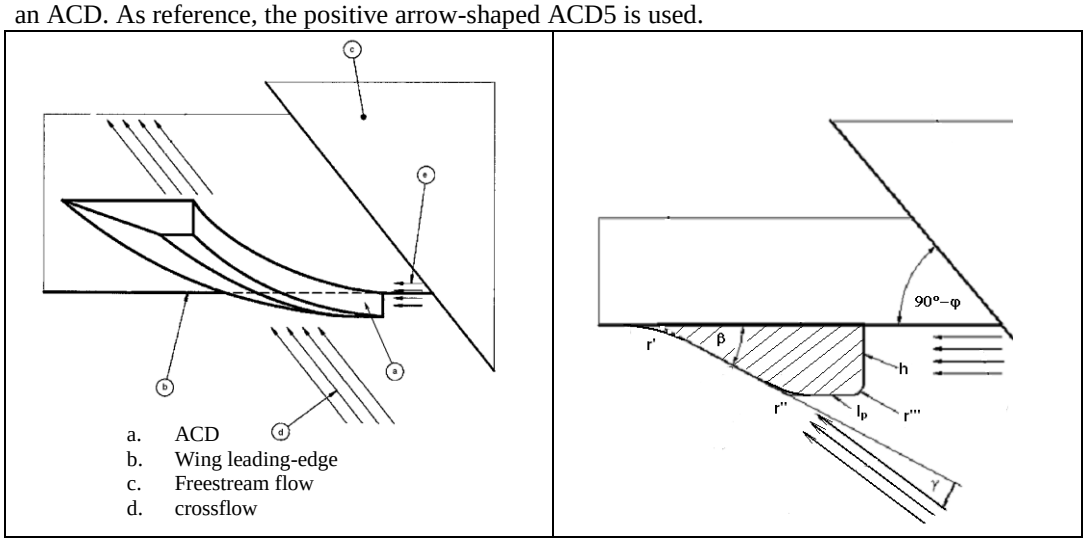

Figure 10:

The main parameters of the ACD for dimensioning purpose are ACD-height h, length of plateau l_p and rearface included angle β. Other parameters are the radius of the leading edge R, radius r_A of the ACD-nose (apex) and some filleting radius r´, r´ and r´´´ at the corners of the ACD. Some thought for predicting main parameters are presented below. The predictions are based on common engineering principles as well as on basic equations of fluid mechanics and boundary layers, especially regarding continuity momentum-, and energy equations in their for-this-purpose required form.

Nose radius

The most important parameter is the **nose radius r** (radius of half cylinder). It is determined by the requirements of the ACD based on cruising flight data. These include cruise altitudes, cruise speed and cruise angle-of-attack range. If the objective is to configure the ACD for a fixed design point at a given angle of attack α, a very small nose radius can be chosen, so much that mechanical

erosion and abrasion are no longer an issue. If the ACD is to be dimensioned for an angle-of-attack range, either the radius can be made larger to cover the angle-of-attack range, or less favourable asymmetric flow over ACD is accepted. The first approach is preferred for the ACD-design.

Height of device

The **height of the device h** is predicted as follows. It depends on the front face width b, which is the ACD nose diameter d i.e. b = d. For increasing the nose radius r_A, turbulent flow accumulation in front of the device increases and the height should be higher (and vice versa). At $r_A \rightarrow \infty$ the device turns in a flat wall and for this condition height is theoretically infinite. In practice the height is going to get a maximum value h_M. In font of the device the intensity of turbulence is substantially higher. If r_A=0 and the height of boundary layer thickness equals δ:

$$r_A = 0 \Rightarrow h = \delta \text{ and}$$

$$r_A \rightarrow \infty \Rightarrow h = \infty .$$

A simple empirical formula can be introduced

$$\frac{h}{\delta} = A\frac{r_A}{\delta} + 1,$$

which fulfils both, maximum-height requirement (infinite) as well as zero- height requirement. In this case, constant *A* stands for a constant which has to be determined. It is also to notice that the ACD-height should also consider the pressure loss, which is reflected by the expression:

$$\Delta p_{ACD} = \varsigma\rho\frac{W_e^2}{2},$$

where ζ is the drag coefficient and W_e the B.L. edge velocity. The higher the resistance of ACD-nose, the more turbulent fluid flow will be transported aside of the ACD. There is also a dependency between ACD-height and resistance (or drag). Thus, one may consider the drag coefficient ζ as a parameter for determining the ACD-height:

$$h = f(\varsigma, r_A, \delta).$$

The drag coefficient ζ depends on the form factor h/r_A of the nose (half cylinder):

$$\varsigma = f_1(h, r_A) = f\left(\frac{h}{r_A}\right)$$

A dependency of the ACD height to $\overline{R}^*$ was also taken into consideration. This issue is however still open because no proven results are available. However, it can be deduced from the wind tunnel experiment. The ACD5 has a height of 5 mm and was tested at M=1.7 as well as M=2.7 and at total pressure between 0.3 bar and 1.4 bar. It was shown that at M=1.7 the device worked effectively up to a total pressure of ca. 0.52-0.58 bar and at M=2.7 up to a total pressure of ca. 1.2-1.25 bar. It was supposed that at these conditions the turbulence thickness just crossed over the ACD. To this turbulence thickness there is a corresponding $\overline{R}^*$**.** Hence, the following problem can be formulated: An equivalent thickness should be found, which is connected to the turbulence intensity or turbulence transport and which results about 5 mm for the above mentioned conditions. This equivalent thickness should be higher as $\overline{R}^*$ gets higher.

Rear slope angle

Due to design aspects the **rear slope angle** β could be about 2-3° smaller (see *fig. 7*) than the included angle between airspeed and wing leading-edge (90°-φ):

$$\beta = \frac{\pi}{2} - \varphi - \varepsilon \text{, with } \varepsilon = 2\text{-}3°.$$

This value leads to a smaller value for the length of ACD. In order to achieve a very smooth passage to the wing surface, one may use the value:

$$\beta_{opt} \cong 6^{o}.$$

This value is independent of the wing sweep angle φ and leads to a bigger value for the length of ACD.

Length of plateau

The **length of the plateau l_P** is significant for 'positive'-arrow-shaped ACD. It depends on the rounding radii at the plateau-edges r´´ and r´´´, and the rear slope angle β. Minimum length is given by the following formula:

$$l_P \geq r''' + r'' \sin\frac{\beta}{2}.$$

Transition radius

The transition radius r´ between ACD and wing surface is of essential significance for the loss-free forwarding of the new laminar boundary layer. Its dimension is bounded by the following relation:

$$r' + r'' \leq \frac{l_P + h \cdot ctg\beta - r'''}{\sin\beta}.$$

Miscellaneous

Due to the fact that the height of the device has a small rounding at the top side (r_S=0.5 mm) and has to cover also boundary layer fluctuations, the height of the device should contain a security margin of 25 to 30%.

6 CONCLUSIONS

Several ACD-shapes and basic guidelines for their optimization have been presented. In the following, some conclusions are drawn. The problem of anti-contamination is a local problem of de-contamination. The ACD just stops and removes the contaminated flow from the leading edge and conducts it downstream to upper and lower wing surface. As consequence, the use of RANS methods is justified and completely sufficient, since a simulation of the re-laminarisation process is not stringently required. The quality of an ACD can then be evaluated by its turbulent level i.e. viscosity ratio, streamlines and pressure distribution. Investigations on simple ACD-shapes delivered a trapezoidal cross-section as a promising solution for ACD. However, since the device had also to provide minimum disturbance, a unique arrow-shaped ACD was introduced. The ACD5 was the positive arrow-shaped ACD which was then proven to be effective experimentally. Its negative counter-part was also designed and expected to generate even less disturbance. Another type of ACD, the split-ACD was conceived and has the characteristics to prevent the contaminated boundary layer on the fuselage from being propagated spanwise by letting it flow smoothly downward trough wing root.

In order to be efficient, an ACD should be designed according to the given cruise flight conditions. It should also be optimized concerning its energy losses. The ACD contour has to follow the streamlines at the clean leading edge. The apex radius is determined to cope with the range of the cruise incidences. It is to remind that the larger the radius, the larger also the energy losses and its disturbance, caused by flow stagnation in front of the apex. Hence, the apex radius determines, in turn, the height of ACD in such way that the turbulence is prevented from crossing-over the ACD. The slope of the rear face is an important specific parameter of this ACD since the flow behind of ACD should be laminar. Furthermore, corner edges should be rounded or filleted to

allow smooth streamlines and to avoid any local vortices over ACD. Finally the effective ACD should exhibit smooth streamlines over the ACD in general; high-turbulent layer or streamlines must not cross over the head of ACD and minimum flow disturbance (i.e. pressure and vortices) of the flow around the ACD is to be achieved.

The knowledge on ACD however has not matured yet. There are still open problems e.g. regarding experimental validation, basic theory and some variables which may affect its effectiveness such as shock wave, attachment line Reynolds number etc.

References

[1] Smith, A. and Poll, D.I.A.: "Instability and Transition Flow at and near an Attachment Line, including Control by Surface Suction", NASA / CR - 1998 – 208443, July 1998.

[2] Pfenninger, W.: "Flow Phenomena at the Leading Edge of Swept Wing", Some results from the X-21 Program, Part I, 1965.

[3] Gaster, M.: "A Simple Device for Preventing Turbulent Contamination on Swept Leading Edges", Technical Note, p788-789.

[4] Creel, T.R.: "Effect of Sweep Angle and Passive Relaminarization Devices on Supersonic Swept-Cylinder Boundary Layer", AIAA - 91 – 0066, January 1991.

[5] Krier, J.V., Sucipto, T., Donelli, R., Godard, J.L, Viscatt, P., Zanazzi, G.: "Numerical Investigation of Leading Edge Anti Contamination Devices In Supersonic Flow", SUPERTRAC project document, 2005

[6] Arnal, D. & all: "Detail review of S2MA Wind tunnel data and comparison with numerical results", SUPERTRAC project document, 2007

[7] Krier, J.V., Sucipto, T.: "Anti Contamination Device Swept Wing Aircraft", HME-Conference, Timisoara, Romania, 2008

[8] Krier, J.V.: "Grenzschichtbetrachtungen für ACD Design", IBK 363i-09, IBK internal report, Nürnberg, Jan. 2008

[9] Krier, J.V., Sucipto, T.: "Passive and Active Device for Laminar Flow Control", KATnet II Conference, Bremen, 2009